



UvA-DARE (Digital Academic Repository)

Physical parametres of GRB 970508 and GRB 971214 from their afterglow synchrotron emission

Wijers, R.A.M.J.; Galama, T.J.

Published in:
Astrophysical Journal

DOI:
[10.1086/307705](https://doi.org/10.1086/307705)

[Link to publication](#)

Citation for published version (APA):

Wijers, R. A. M. J., & Galama, T. J. (1999). Physical parametres of GRB 970508 and GRB 971214 from their afterglow synchrotron emission. *Astrophysical Journal*, 523, 177-186. DOI: 10.1086/307705

General rights

It is not permitted to download or to forward/distribute the text or part of it without the consent of the author(s) and/or copyright holder(s), other than for strictly personal, individual use, unless the work is under an open content license (like Creative Commons).

Disclaimer/Complaints regulations

If you believe that digital publication of certain material infringes any of your rights or (privacy) interests, please let the Library know, stating your reasons. In case of a legitimate complaint, the Library will make the material inaccessible and/or remove it from the website. Please Ask the Library: <http://uba.uva.nl/en/contact>, or a letter to: Library of the University of Amsterdam, Secretariat, Singel 425, 1012 WP Amsterdam, The Netherlands. You will be contacted as soon as possible.

PHYSICAL PARAMETERS OF GRB 970508 AND GRB 971214 FROM THEIR AFTERGLOW SYNCHROTRON EMISSION

R. A. M. J. WIJERS¹ AND T. J. GALAMA²

Received 1998 May 26; accepted 1999 April 29

ABSTRACT

We have calculated synchrotron spectra of relativistic blast waves and find predicted characteristic frequencies that are more than an order of magnitude different from previous calculations. For the case of an adiabatically expanding blast wave, which is applicable to observed gamma-ray burst (GRB) afterglows at late times, we give expressions to infer the physical properties of the afterglow from the measured spectral features. We show that enough data exist for GRB 970508 to compute unambiguously the ambient density, $n = 0.03 \text{ cm}^{-3}$, and the blast wave energy per unit solid angle, $\mathcal{E} = 3 \times 10^{52} \text{ ergs}/4\pi \text{ sr}$. We also compute the energy density in electrons and magnetic field. We find that they are 12% and 9%, respectively, of the nucleon energy density and thus confirm for the first time that both are close to but below equipartition. For GRB 971214, we discuss the break found in its spectrum by Ramaprakash et al. It can be interpreted either as the peak frequency or as the cooling frequency; both interpretations have some problems, but on balance the break is more likely to be the cooling frequency. Even when we assume this, our ignorance of the self-absorption frequency and presence or absence of beaming make it impossible to constrain the physical parameters of GRB 971214 very well.

Subject headings: gamma rays: bursts — gamma rays: theory — radiation mechanisms: nonthermal — shock waves

1. INTRODUCTION

Explosive models of gamma-ray bursts (GRBs), in which relativistic ejecta radiate away some of their kinetic energy as they are slowed down by swept-up material, naturally lead to a gradual softening of the emission at late times. This late-time softer radiation has been dubbed the “afterglow” of the burst, and its strength and time dependence were predicted theoretically (Mészáros & Rees 1997). Soon after this prediction, the accurate location of GRB 970228 by the *BeppoSAX* satellite’s Wide Field Cameras (Piro, Scarsi, & Butler 1995; Jager et al. 1995) enabled the detection of the first X-ray and optical afterglow (Costa et al. 1997b; van Paradijs et al. 1997). Its behavior agreed well with the simple predictions (Wijers, Rees, & Mészáros 1997; Waxman 1997a; Reichart 1997).

The basic model is a point explosion with an energy of order 10^{52} ergs, which expands with high Lorentz factor into its surroundings. As the mass swept up by the explosion begins to be significant, it converts its kinetic energy to heat in a strong shock. The hot, shocked matter acquires embedded magnetic fields and accelerated electrons, which then produce the radiation we see via synchrotron emission. The phenomenon is thus very much the relativistic analog of supernova remnant evolution, played out apparently in seconds owing to the strong time contractions resulting from the high Lorentz factors involved. Naturally, the Lorentz factor of the blast wave decreases as more matter is swept up, and consequently the power output and typical energy decrease with time after the initial few seconds of gamma-ray emission. This produces the X-ray afterglows, which have been detected up to 10 days after the burst (Frontera et al. 1998), and the optical ones, which have been detected up to a year after the burst (Fruchter et al. 1997; Bloom et al. 1998a; Castro-Tirado et al. 1998).

The burst of 1997 May 8 was bright for a relatively long time and produced emission from gamma rays to radio. This enabled a detailed analysis of the expected spectral features of a synchrotron spectrum, confirming in great detail that we are indeed seeing synchrotron emission and that the dynamical evolution of the expanding blast wave agrees with predictions if the blast wave dynamics are adiabatic (Galama et al. 1998a, 1998b). In principle, one can derive the blast wave properties from the observed synchrotron spectral features. The problem is that the characteristic synchrotron frequencies and fluxes are taken from simple dimensional analysis in the published literature, so they are not suitable for detailed data analysis. Since there are now enough data on the afterglows of a few GRBs to derive their physical properties, we amend this situation in § 2, correcting the coefficients in the equations for the break frequencies by up to a factor 10. We then use our theoretical results to infer the physical properties of the afterglows of GRB 970508 (§ 3) and attempt the same for GRB 971214 (§ 4). We conclude with a summary of results and discuss some prospects for future improvements in observation and analysis (§ 5).

2. RADIATION FROM AN ADIABATIC BLAST WAVE

2.1. Blast Wave Dynamics

We rederive the equations for synchrotron emission from a blast wave in order to clean up some imprecisions in previous versions. Since the dynamical evolution of the blast waves should be close to adiabatic after the first hour or so, we specialize

¹ Institute of Astronomy, Madingley Road, Cambridge CB3 0HA, UK; and Department of Physics and Astronomy, State University of New York, Stony Brook, NY 11794-3800.

² Astronomical Institute “Anton Pannekoek,” University of Amsterdam; and Center for High Energy Astrophysics, Kruislaan 403, 1098 SJ Amsterdam, The Netherlands.

to the case of dynamically adiabatic evolution. This means that the radius r and Lorentz factor γ evolve with observer time as (Rees & Mészáros 1992; Mészáros & Rees 1997; Waxman 1997a; Wijers et al. 1997)

$$r(t) = r_{\text{dec}}(t/t_{\text{dec}})^{1/4} \quad (1)$$

$$\gamma(t) = \eta(t/t_{\text{dec}})^{-3/8}. \quad (2)$$

Here $\eta \equiv E/M_0 c^2$ is the ratio of initial energy in the explosion to the rest mass energy of the baryons (mass M_0) entrained in it, the deceleration radius r_{dec} is the point where the energy in the hot, swept-up interstellar material equals that in the original explosion, and t_{dec} is the observer time at which the deceleration radius is reached. Denoting the ambient particle number density as n , in units of cm^{-3} , we have

$$\begin{aligned} r_{\text{dec}} &= \left(\frac{E}{4\pi\eta^2 n m_p c^2} \right)^{1/3} \\ &= 1.81 \times 10^{16} \left(\frac{E_{52}}{n} \right)^{1/3} \eta_{300}^{-2/3} \text{ cm} \end{aligned} \quad (3)$$

$$t_{\text{dec}} = \frac{r_{\text{dec}}}{2\eta^2 c} = 3.35 \left(\frac{E_{52}}{n} \right)^{1/3} \eta_{300}^{-8/3} \text{ s}, \quad (4)$$

with m_p the proton mass and c the speed of light, and we have normalized to typical values: $E_{52} = E/10^{52}$ ergs and $\eta_{300} = \eta/300$. Strictly speaking, we have defined n here as $n \equiv \rho/m_p$, where ρ is the ambient rest mass density. Setting $t_d = t/1$ day we then have, for $t > t_{\text{dec}}$,

$$r(t) = 2.29 \times 10^{17} (E_{52}/n)^{1/4} t_d^{1/4} \text{ cm} \quad (5)$$

$$\gamma(t) = 6.65 (E_{52}/n)^{1/8} t_d^{-3/8}. \quad (6)$$

Note that neither γ nor r depend on η : once the blast wave has entered its phase of self-similar deceleration, its initial conditions have been partly forgotten. The energy E denotes the initial blast wave energy; it and the ambient density do leave their marks. It should also be noted that these equations remain valid in an anisotropic blast wave, where the outflow is in cones of opening angle θ around some axis of symmetry, as long as its properties are uniform within the cone and the opening angle is greater than $1/\gamma$ (Rhoads 1998). We should then replace E by the equivalent energy per unit solid angle $\mathcal{E} \equiv E/\Omega$. To express this equivalence we shall write the normalization for this case as $\mathcal{E}_{52} = \mathcal{E}(4\pi/10^{52} \text{ ergs})$, so we can directly replace E_{52} in all equations with \mathcal{E}_{52} to convert from the isotropic to the anisotropic case.

Before we can calculate the synchrotron emission from the blast wave, we have to compute the energies in electrons and magnetic field (or rather, summarize our ignorance in a few parameters). First, we assume that electrons are accelerated to a power-law distribution of Lorentz factors, $N(\gamma_e) \propto \gamma_e^{-p}$, with some minimum Lorentz factor γ_m . We are ignorant of what p should be, but it can in practice be determined from the data. The total energy in the electrons is parameterized by the ratio, ϵ_e , of energy in electrons to energy in nucleons. This is often called the electron energy fraction, but that term is only appropriate in the limit of small ϵ_e . The postshock nucleon thermal energy is $\gamma m_p c^2$, and the ratio of nucleon to electron number densities is the same as the preshock value, which we can parameterize as $2/(1+X)$, where X is the usual hydrogen mass fraction. In terms of these we have

$$\epsilon_e \equiv \frac{n_e \langle E_e \rangle}{n \gamma m_p c^2} = \frac{1+X}{2} \frac{m_e p - 1}{m_p p - 2} \frac{\gamma_m}{\gamma} \quad (7)$$

$$\gamma_m = \frac{2}{1+X} \frac{m_p p - 2}{m_e p - 1} \epsilon_e \gamma. \quad (8)$$

The strength of the magnetic field in the comoving frame is parameterized by setting the field energy density, $B'^2/8\pi$, to a constant fraction, ϵ_B , of the postshock nucleon energy density $e' = 4\gamma^2 n m_p c^2$. (Primed quantities are measured in the rest frame of the shocked, swept-up material; others are measured in the frame of an observer outside the blast wave at rest relative to the explosion center.) Consequently,

$$\begin{aligned} B' &= \gamma c \sqrt{32\pi n m_p \epsilon_B} \\ &= 2.58 \epsilon_B^{1/2} \mathcal{E}_{52}^{1/8} n^{3/8} t_d^{-3/8} \text{ G}. \end{aligned} \quad (9)$$

From the above relations, we can express the evolution of the synchrotron spectrum from the blast wave in terms of observable quantities and six unknown parameters: \mathcal{E}_{52} , n , X , p , ϵ_e , and ϵ_B . But first we need to relate the synchrotron spectrum to these parameters.

2.2. Synchrotron Radiation

We now derive the correct synchrotron frequencies and fluxes. These are strictly valid only for a uniform medium moving with a constant Lorentz factor. Real blast waves decelerate, of course, and have a more complicated structure behind the shock. The blast wave deceleration means that surfaces of constant arrival time are no longer the ideal ellipses expected for a constant speed of the blast wave (Rees 1966), and at a given time we see contributions from gas with different Lorentz factors.

This effect has been discussed thoroughly (Waxman 1997b; Panaitescu & Mészáros 1998; Sari 1998). The uniformity behind the shock is also a simplification: in reality the Lorentz factor varies from just behind the shock to the contact discontinuity. The density and other parameters vary accordingly (Blandford & McKee 1976). This effect has not yet been treated; it is expected to be comparable in importance to deceleration. Since both these effects are rather less important than our corrections to the synchrotron frequencies, we shall neglect both rather than attempt to apply only one of them. However, our improved treatment of the synchrotron emission is purely local and can be incorporated into any formalism that accounts for the varying local properties of the shocked medium at a fixed observer time.

We assume that the electron population in any local volume has an isotropic distribution of angles relative to the magnetic field and that the magnetic field is sufficiently tangled that we may average the emission properties assuming a random mix of orientation angles between the field and our line of sight. The radiated power per electron per unit frequency, integrated over emission angles is

$$P' \left(\frac{\nu}{v_{\perp}(\gamma_e)}, \alpha \right) = \frac{\sqrt{3} e^3 B' \sin \alpha}{m_e c^2} F \left(\frac{\nu}{v_{\perp} \sin \alpha} \right) \text{ ergs cm}^{-2} \text{ s}^{-1} \text{ Hz}^{-1} \text{ electron}^{-1}, \quad (10)$$

where F is the standard synchrotron function (e.g., Rybicki & Lightman 1979), and e and m_e are the electron charge and mass. α is the angle between the electron velocity and the magnetic field, and

$$v_{\perp}(\gamma_e) = \frac{3\gamma_e^2 e B'}{4\pi m_e c}. \quad (11)$$

(i.e., the traditional characteristic synchrotron frequency equals $v_{\perp} \sin \alpha$ in our notation.) Next, we define the isotropic synchrotron function F_{iso} by averaging over an isotropic distribution of α . Setting $x_{\perp}(\gamma_e) = \nu/v_{\perp}(\gamma_e)$, we get

$$P'_{\text{iso}}(x_{\perp}) = \frac{\sqrt{3} e^3 B'}{m_e c^2} F_{\text{iso}}(x_{\perp}) \text{ ergs cm}^{-2} \text{ s}^{-1} \text{ Hz}^{-1} \text{ electron}^{-1} \quad (12)$$

$$F_{\text{iso}}(x_{\perp}) = \int_0^{\pi/2} d\alpha \sin^2 \alpha F(x_{\perp}/\sin \alpha) \quad (13)$$

(We have made use of the symmetry of $\sin \alpha$ to absorb a factor 1/2 into confining the integral to the first quadrant. The apparent singularity at $\alpha = 0$ poses no problems because F decreases exponentially for large values of the argument.) Note that most calculations of blast wave spectra assume that the spectrum peaks at frequency $\gamma_e^2 e B'/m_e c$. Owing to the neglect of the factor $3/4\pi$ and the fact that $F(x)$ peaks at $x = 0.28587$ and $F_{\text{iso}}(x)$ at $x = 0.22940$, this estimate leads to quite erroneous inferences about blast wave properties.

Finally, we must average the emission over a distribution of electron energies. We assume a simple power-law probability distribution of electrons between extreme values γ_m and γ_t :

$$f(\gamma_e) = \frac{f_0}{\gamma_m} \left(\frac{\gamma_e}{\gamma_m} \right)^{-p} \quad \gamma_m \leq \gamma_e \leq \gamma_t \quad (14)$$

$$f_0 = \frac{p-1}{1 - (\gamma_t/\gamma_m)^{1-p}}. \quad (15)$$

Now let $x = \nu/v_{\perp}(\gamma_m)$. Then the average power per electron becomes

$$P'_{\text{PL}}(x) = \frac{\sqrt{3} e^3 B'}{m_e c^2} F_{\text{PL}}(x) \text{ ergs cm}^{-2} \text{ s}^{-1} \text{ Hz}^{-1} \text{ electron}^{-1} \quad (16)$$

$$F_{\text{PL}}(x) = \frac{f_0}{2} x^{-(p-1)/2} \int_{x\gamma_m^2/\gamma_t^2}^x du u^{(p-3)/2} F_{\text{iso}}(u), \quad (17)$$

in which we have transformed the integration variable from γ_e to $u \equiv x\gamma_m^2/\gamma_e^2$. The last equation shows the familiar result that for $1 \lesssim x \lesssim \gamma_t^2/\gamma_m^2$ the spectrum from a power law of electrons is itself a power law. Since this region is known to extend over many decades in GRB and afterglow spectra, we quote numerical results for the case $\gamma_t \gg \gamma_m$, for which the quoted results are independent of γ_t . The most easily identified point in the spectrum is its dimensionless maximum, x_p , and the dimensionless flux at this point, $F_{\text{PL}}(x_p) \equiv \phi_p$; their dependence on p is shown in Figure 1. Both now depend on the electron energy slope p . This defines the first two numbers that we can measure in the spectrum:

$$v'_m = x_p v_{\perp}(\gamma_m) = \frac{3x_p \gamma_m^2 e B'}{4\pi m_e c} \quad (18)$$

$$P'_{v_m} = \phi_p \frac{\sqrt{3} e^3 B'}{m_e c^2}. \quad (19)$$

The calculation of the break frequency ν_c that separates radiation from slowly and rapidly cooling electrons (Sari, Piran, & Narayan 1998) is somewhat more difficult because the cooling rate depends on both γ_e and pitch angle α . However, since the cooling and the emission are both dominated by $\alpha = \pi/2$, we may estimate the break as the peak of $F(x)$ for the value of γ_e

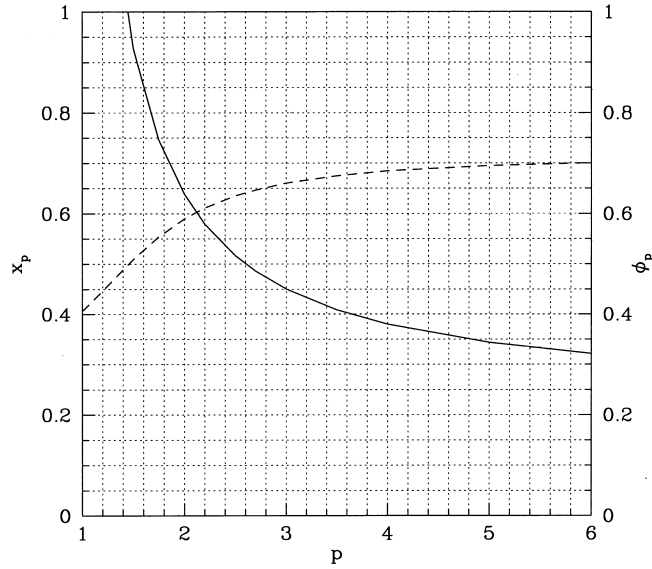


FIG. 1.—Dimensionless location x_p (solid line) and dimensionless peak flux ϕ_p (dashed line) of a synchrotron spectrum from a power law of electrons, as a function of the power-law index, p , of the electron energy distribution.

where the cooling time for electrons with $\alpha = \pi/2$ equals the expansion time, t :

$$\gamma_c = \frac{6\pi m_e c}{\sigma_T \gamma B'^2 t} \quad (20)$$

$$\nu'_c = 0.286 \frac{3}{4\pi} \frac{\gamma_c^2 e B'}{m_e c}. \quad (21)$$

In order to transform frequency and power from the rest frame of the emitting material to our frame, we note that the emission is isotropic in the rest frame by assumption. It is then trivial to compute the angle-average Doppler factors (see Rybicki & Lightman 1979, chap. 4). For the received power, we find $P = \gamma^2(1 + \beta^2/3)P'$, which we shall simplify to $P = 4\gamma^2 P'/3$ in keeping with the fact that our whole treatment is done in the ultrarelativistic limit, $\beta \rightarrow 1$. Similarly, the intensity-weighted mean change in any frequency is $\nu = 4\gamma\nu'/3$. Consequently, the appropriate mean of a power per unit frequency will transform as $P_\nu = \gamma P'_\nu$. Of course, the spectrum also gets broadened, but that will not affect the locus of characteristic frequencies significantly.

The synchrotron self-absorption frequency is usually set at the point where $\tau_\nu = 0.35$. Using the comoving width of the shock, $\Delta r' = r/4\gamma$, and the expression for the synchrotron absorption coefficient (Rybicki & Lightman 1979), we get

$$\nu_a = \frac{4\gamma\nu'_a}{3} = 2.97 \times 10^8 [(p+2)/p + 2/3]^{3/5} (p-1)^{8/5} / (p-2)(1+X)^{8/5} n^{3/5} \epsilon_e^{-1} \epsilon_B^{1/5} \mathcal{E}_{52}^{1/5} (1+z)^{-1} \text{ Hz}, \quad (22)$$

where we have used equations (5)–(9) for the blast wave dynamics to express ν_a in terms of the unknowns we try to solve for, and have added the correction for redshift, i.e., the equation in this form relates the observed frequency on Earth to the properties of the blast wave measured by a local observer at rest relative to the center of the explosion. Note that the self-absorption frequency in this simplest form is time-independent. We now also translate the other two frequencies into practical form:

$$\nu_m = 4\gamma\nu'_m/3 = 5.73 \times 10^{16} x_p [(p-2)/(p-1)]^2 \epsilon_e^2 \epsilon_B^{1/2} \mathcal{E}_{52}^{1/2} (1+X)^{-2} (1+z)^{1/2} t_d^{-3/2} \text{ Hz} \quad (23)$$

$$\nu_c = 4\gamma\nu'_c/3 = 1.12 \times 10^{12} \epsilon_B^{-3/2} \mathcal{E}_{52}^{-1/2} n^{-1} (1+z)^{-1/2} t_d^{-1/2} \text{ Hz}. \quad (24)$$

Note the nontrivial redshift dependence of both, which stems from the fact that t_d is also measured on Earth and therefore redshifted. The observed flux at ν_m can be obtained by noting that our assumption of uniformity of the shocked material means that all swept-up electrons since the start contribute the same average power per unit frequency at ν_m (at any frequency, in fact), which is given by equation (19). Adding one factor of γ to transform to the lab frame and accounting for the redshift, we have

$$F_{\nu_m} = \frac{N_e \gamma P'_{\nu_m} (1+z)}{4\pi d_L^2}, \quad (25)$$

where N_e is the total number of swept-up electrons, related to the blast wave parameters by $N_e = (4\pi/3)r^3 n(1+X)/2$. The luminosity distance depends on cosmological parameters and for an $\Omega = 1$, $\Lambda = 0$ universe, which we shall adopt here, is

given by $d_L = 2c(1+z - \sqrt{1+z})/H_0$. Consequently,

$$F_{\nu_m} = 1.15 \frac{h_{70}^2}{(\sqrt{1+z} - 1)^2} \phi_p (1+X) \mathcal{E}_{52} n^{1/2} \epsilon_B^{1/2} \text{ mJy}, \quad (26)$$

where $h_{70} = H_0/70 \text{ km s}^{-1} \text{ Mpc}^{-1}$.

Equations (22), (23), (24), and (26) now are four independent relations between the four parameters of interest \mathcal{E}_{52} , n , ϵ_e , and ϵ_B . This means we can solve for all parameters of interest if we have measured all three break frequencies (not necessarily at the same time) and the peak flux of the afterglow. In addition this requires us to know the redshift of the burst, the electron index p , and the composition parameter, X , of the ambient medium. Note that multiple measurements of the same break at different times serve to test the model assumptions but do not provide extra constraints on the parameters, since validity of the model implies that any of the four key equations is satisfied for all time if it is satisfied once. We therefore define the constants $C_a \equiv v_a/v_{a*}$, $C_m \equiv v_m t_{dm}^{3/2}/v_{m*}$, $C_c \equiv v_c t_{dc}^{1/2}/v_{c*}$, and $C_F = F_{\nu_m}/F_{\nu_{m*}}$. Here starred symbols denote the numerical coefficients in each of the four equations, and times denote the time at which the quantity in question was measured. Rearranging the four equations then yields

$$\mathcal{E}_{52} = C_a^{-5/6} C_m^{-5/12} C_c^{1/4} C_F^{(3/2)3/2} x_p^{5/12} \phi_p^{-3/2} (p-1)^{1/2} \left[\frac{p+2}{p+1/2} \right]^{1/2} (1+X)^{-1} (1+z)^{-1/2} \left(\frac{\sqrt{1+z}-1}{h_{70}} \right)^3 \quad (27)$$

$$\epsilon_e = C_a^{5/6} C_m^{11/12} C_c^{1/4} C_F^{-1/2} x_p^{-11/12} \phi_p^{1/2} \left[\frac{(p-1)^{1/2}}{p-2} \right] \left[\frac{p+2}{p+1/2} \right]^{-1/2} (1+X)(1+z)^{1/2} \left(\frac{\sqrt{1+z}-1}{h_{70}} \right)^{-1} \quad (28)$$

$$\epsilon_B = C_a^{-5/2} C_m^{-5/4} C_c^{-5/4} C_F^{1/2} x_p^{5/4} \phi_p^{-1/2} (p-1)^{3/2} \left[\frac{p+2}{p+3/2} \right]^{3/2} (1+X)(1+z)^{-5/2} \left(\frac{\sqrt{1+z}-1}{h_{70}} \right) \quad (29)$$

$$n = C_a^{25/6} C_m^{25/12} C_c^{3/4} C_F^{-3/2} x_p^{-25/12} \phi_p^{3/2} (p-1)^{-5/2} \left[\frac{p+2}{p-5/2} \right]^{-5/2} (1+X)^{-1} (1+z)^{7/2} \left(\frac{\sqrt{1+z}-1}{h_{70}} \right)^{-3}. \quad (30)$$

The last factor in each of these stems from the specific cosmological model adopted, and has entered the solution only via equation (25). To generalize to any cosmology, all that is needed is to replace $(\sqrt{1+z}-1)/h_{70}$ in the above equations by $(d_L/8.57 \text{ Gpc})/\sqrt{1+z}$.

3. OBSERVED AND INFERRED PARAMETERS OF GRB 970508

GRB 970508 was a moderately bright gamma-ray burst (Costa et al. 1997b; Kouveliotou et al. 1997). It was detected on May 8.904 UT with the Gamma-Ray Burst Monitor (GRBM; Frontera et al. 1991), and with the Wide Field Cameras (WFCs; Jager et al. 1995) on board the Italian-Dutch X-ray observatory *BeppoSAX* (Piro et al. 1995). Optical observations of the WFC error box (Heise et al. 1997a), made on May 9 and 10, revealed a variable object at R.A. = 06^h53^m49^s.2, decl. = +79°16'19" (J2000), which showed an increase by ~ 1 mag in the V band (Bond 1997). *BeppoSAX* Narrow Field Instrument observations revealed an X-ray transient (Piro et al. 1997), the position of which is consistent with that of the optical variable, and Frail et al. (1997) found the first GRB radio afterglow for GRB 970508; the radio source position coincides with that of the optical source (Bond 1997).

The spectrum of the optical variable showed absorption lines at redshifts 0.77 and 0.835, indicating that 0.835 is the minimum redshift of the afterglow (Metzger et al. 1997a, 1997b). Subsequently, an [O II] emission line with $z = 0.835$ was also found in the host's spectrum (Bloom et al. 1998a), which is often associated with star-forming regions in galaxies. A faint underlying galaxy or star-forming region is inferred to indeed exist from a levelling off of the light curve after 6–11 months (Bloom et al. 1998a; Castro-Tirado et al. 1998). It must be very compact, since the *Hubble Space Telescope* limits on an extended object underlying the GRB are fainter than the magnitude inferred from the light curve (Pian et al. 1998). It is therefore almost certain that the compact nebula is the source of the [O II] line and therefore also of the majority of the absorption lines. Given its compactness, a chance location of the burst far behind it is unlikely, and we shall assume that the burst occurred in this nebula, i.e., its redshift is 0.835.

From the light-curve behavior and broadband spectrum (Fig. 2) of GRB 970508, Galama et al. (1998a, 1998b) deduced the other properties of the burst required to calculate the physical parameters of the afterglow. We summarize them here: at $t = 12.1$ days after trigger, the break frequencies are $\nu_a = 2.5 \times 10^9$ Hz, $\nu_m = 8.6 \times 10^{10}$ Hz, and $\nu_c = 1.6 \times 10^{14}$ Hz. The peak flux is $F_{\nu_m} = 1.7$ mJy and the electron index $p = 2.2$. After the first 500 s, electrons no longer cooled efficiently, and the afterglow must evolve adiabatically. We shall set the cosmological parameters to be $\Omega = 1$, $\Lambda = 0$, $H_0 = 70 \text{ km s}^{-1} \text{ Mpc}^{-1}$. As noted above, they enter the solution only via the luminosity distance, and alternatives can therefore be incorporated easily via the substitution given following equation (30). Finally, we adopt $X = 0.7$ for the composition of the ambient medium. There are no reasons in the model to assume the ambient medium would not have normal cosmic abundance. While the metallicity Z is a strong function of redshift, X is hardly redshift-dependent, since the balance between H and He in cosmic matter has not been changed very much by nucleosynthesis. Using further that $x_{2.2} = 0.580$, $\phi_{2.2} = 0.611$, we find

$$\mathcal{E}_{52} = 3.5, \quad n = 0.030, \quad \epsilon_e = 0.12, \quad \epsilon_B = 0.089. \quad (31)$$

We do note once more our deliberate use of \mathcal{E}_{52} , the energy per unit solid angle scaled to that of an isotropic explosion of 10^{52} ergs, instead of the total energy: \mathcal{E}_{52} is truly constrained by the data, whereas the total energy requires us to know the as yet poorly constrained beaming of bursts. The recent findings by Fruchter et al. (1999a) suggest there might be a break in the late

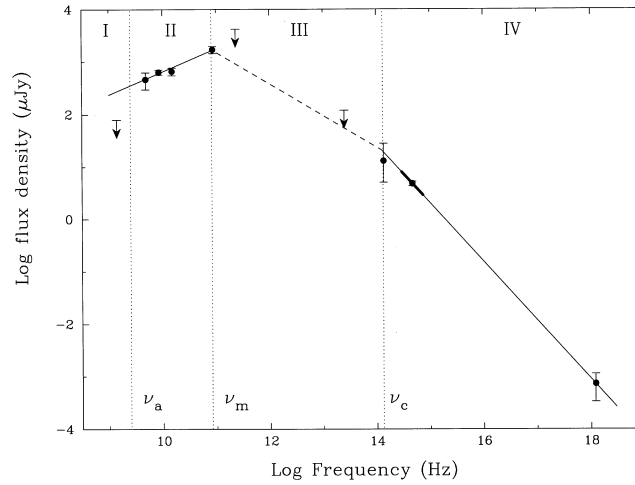


FIG. 2.—X-ray-to-radio spectrum of GRB 970508 on May 21.0 UT (12.1 days after the event) from Galama et al. (1998b). Indicated are the inferred values of the break frequencies ν_a , ν_m , and ν_c for May 21.0 UT.

light curve (100–200 days after the burst), at which time the Lorentz factor is 2 or less. If this break is due to beaming, it would be very modest beaming, and the total energy would be only a factor of a few less than the isotropic estimate. Our value of \mathcal{E}_{52} does clearly rule out the very high energy estimates by Brainerd (1998) from the radio data alone. We have demonstrated for the first time that the electron and magnetic field energy densities are indeed close to but somewhat below equipartition. The ambient density is on the low side of normal for a disk of a galaxy but definitely higher than expected for a halo, lending further support to the notion that bursts occur in gas-rich environments. As an aside, we note that switching the values of ν_m and ν_c , which is allowed by the shape of the spectrum at 12.1 days, does not give a sensible solution (e.g., $\epsilon_e = 20$). This confirms the choice of Galama et al. (1998b), who noted that this solution was not compatible with the temporal evolution of the afterglow.

The gamma-ray fluence of GRB 970508 was measured with BATSE to be $(3.1 \pm 0.2) \times 10^{-6}$ ergs cm^{-2} . Using $z = 0.835$ and $h_{70} = 1$, this implies $\mathcal{E}_{52\gamma} = 0.63$. In other words, the energy emitted in gamma rays is 18% of the total blast wave energy (per unit solid angle in our direction). According to Galama et al. (1998b), the afterglow was cooling efficiently until 500 s after trigger; this means that during the gamma-ray phase all the energy given to electrons would be radiated away quickly, and mostly in gamma rays. If this phase is not too long, the energy radiated in gamma rays should be $\mathcal{E}_{52\gamma} = \epsilon_{e\gamma} \mathcal{E}_{52i}$, where $\epsilon_{e\gamma}$ is the value of ϵ_e during the early, gamma-ray-emitting phase and \mathcal{E}_{52i} is the initial value of \mathcal{E}_{52} . Since the subsequent phase will be adiabatic, the blast wave energy measured at late times should be $\mathcal{E}_{52} = (1 - \epsilon_{e\gamma}) \mathcal{E}_{52i}$. Eliminating the initial energy, we conclude that

$$\frac{\epsilon_{e\gamma}}{1 - \epsilon_{e\gamma}} = \frac{\mathcal{E}_{52\gamma}}{\mathcal{E}_{52}}. \quad (32)$$

Therefore the measured ratio of gamma-ray fluence to late-time blast wave energy implies that $\epsilon_{e\gamma} = 0.15$, or slightly greater if some of the initial energy output is at $E < 20$ keV. Compared with $\epsilon_e = 0.12$ at late times, this demonstrates the near-constancy of the fraction of energy that is given to the electrons. Since the inferences about the initial gamma-ray fluence are independent of the whole machinery on blast wave synchrotron emission in the previous section, we may view this agreement as modest evidence that the coefficients derived there are close to correct, despite our simplification of the dynamics.

It is also interesting to compare the properties at late times with those derived from radio observations. The scintillation size after 1 month is about 10^{17} cm (Frail et al. 1997), whereas our formulae give a transverse diameter of 5×10^{17} cm; given the statistical nature of the scintillation size and our neglect of the gradients in properties in the transverse direction, to which this particular measurement is of course sensitive, this is not too bad. The Lorentz factor at this time is 3.4, so the evolution is still just in the ultrarelativistic regime. The field at this time is $B' = 0.07$ G. Katz & Piran (1997) estimated a size of the afterglow of GRB 970508 from a crude measurement of the self-absorption frequency. They found a size of 10^{17} cm, and assuming an ambient density of 1 cm^{-3} , they found that the Lorentz factor had already decreased to 2 and that most of the energy of the blast wave had been lost, i.e. it had evolved with radiative dynamics. The numbers we derive from our full solution after 1 week are $\gamma = 5.8$, transverse diameter $= 2 \times 10^{17}$ cm. This means the blast wave is still quite relativistic, and with our low ambient density there is no need for radiative evolution.

4. PROPERTIES OF GRB 971214

This burst occurred on 1997 December 14.9727 UT. With a fluence of 1.1×10^{-5} ergs cm^{-2} , it is a moderately bright burst (Kippen et al. 1997). After localization by the *BeppoSAX* Wide Field Camera in X-rays (Heise et al. 1997b), the optical afterglow of this burst was found by Halpern et al. (1998). It shows evidence of strong reddening (Halpern et al. 1998; Ramaprakash et al. 1998). Once the afterglow had faded, a host galaxy became visible underneath it, and its redshift was measured to be 3.42 (Kulkarni et al. 1998).

One definite break and another possible one were observed in the spectrum. The definite break (hereafter “optical break”) was found by Ramaprakash et al. (1998); they noted a break in the spectrum of the afterglow at 3×10^{14} Hz, 0.58 days after trigger, in the extinction-corrected *VRIJK* spectrum. Another possible break (hereafter “IR break”) was found by Gorosabel et al. (1998) in *K*-band data 3–5 hr after trigger. In Figure 3 we show the *K*-band light curve. The data are not strongly inconsistent with a pure power-law fit ($\chi^2/\text{dof} = 2.0$) but are suggestive of a break passing through *K* after about 5 hr. The physical interpretation of the afterglow depends rather strongly on whether the optical break is the peak frequency ν_m or the cooling frequency ν_c , so we shall discuss these two cases with their implications and problems in turn.

4.1. The Optical Break as ν_m

Ramaprakash et al. (1998) interpreted the optical break as the peak frequency, ν_m . A complication with the data is that the spectral slope is much too steep to correspond to any simple fireball model, which can be interpreted as due to reddening within the host galaxy (Ramaprakash et al. 1998; Halpern et al. 1998). Since reddening scales approximately as $1/\text{wavelength}$, it cannot be determined without knowing what the true slope of the spectrum is. Assuming a blast wave model, one can predict this slope from the temporal decay rate of the flux and an interpretation of what break is seen. Following Ramaprakash et al., we now assume an adiabatic blast wave and interpret the break as ν_m . Then the flux above the break should depend on frequency and time as $F = F_0 \nu^{-\beta} t^{-\delta}$, where $\beta = 2\delta/3$. There are several determinations of δ , for the *VRI* fluxes: 1.2 ± 0.2 by Kulkarni et al. (1998) and 1.4 ± 0.2 by Halpern et al. (1998). We shall adopt the value 1.3 ± 0.2 in this paper, so $\beta = 0.87 \pm 0.13$ for the case under consideration. The left-hand panel of Figure 4 shows the resulting dereddened spectrum at $t = 0.52$ days (note that Ramaprakash et al. construct the spectrum at a slightly later time, 0.58 days). We find that $\nu_m = 4 \times 10^{14}$ Hz and $F_m = 30 \mu\text{Jy}$. (As an aside, we note that extinction fits with a mean galactic extinction curve are worse, since the redshifted 2200 Å bump falls within *VRI*.) The amount of extinction, 0.43 mag at a rest frame wavelength of 5500 Å, is very modest and does not imply a special location of the burst within the galaxy. A strong point of this fit is that the X-ray flux measured at the same time, which was not included in the fit, agrees nicely with it. The reported nondetections in the radio at levels of 10–50 μJy could be inconsistent with the peak flux: the reddening-corrected F_m is 30 μJy , so we may have to invoke self-absorption to suppress the flux at 8.46 GHz. A weak point is the fact that the flux at *K*, which is below the peak frequency at 0.58 days in this model, would have to rise with time as $t^{1/2}$ as the peak approaches. But the early *K* data by Gorosabel et al. (1998) clearly indicate a significant decline of the flux in *K* from 0.21 to 0.58 days. In fact, the early *K* flux even exceeds the supposed peak flux in the spectrum at 0.52 days, which means the peak flux had to be declining as well. This requires a nonstandard blast wave model (e.g., a beamed one or a nonadiabatic one) and is thus inconsistent with the blast wave model used in this interpretation. Nonetheless, we shall briefly explore the physical implications of this model, since the interpretation of the optical break as a cooling break is not free of problems either.

For the simple adiabatic model used by Ramaprakash et al., we get the blast wave energy from equation (23):

$$\mathcal{E}_{52} = 27 \frac{2}{1+z} \left(\frac{\epsilon_e}{0.2} \right)^{-4} \left(\frac{\epsilon_B}{0.1} \right)^{-1}. \quad (33)$$

The coefficient is 60 times larger than in equation (3) of Ramaprakash et al., almost solely due to our more accurate calculation of the peak frequency. We can use equation (26) to derive an independent estimate of the blast wave energy from

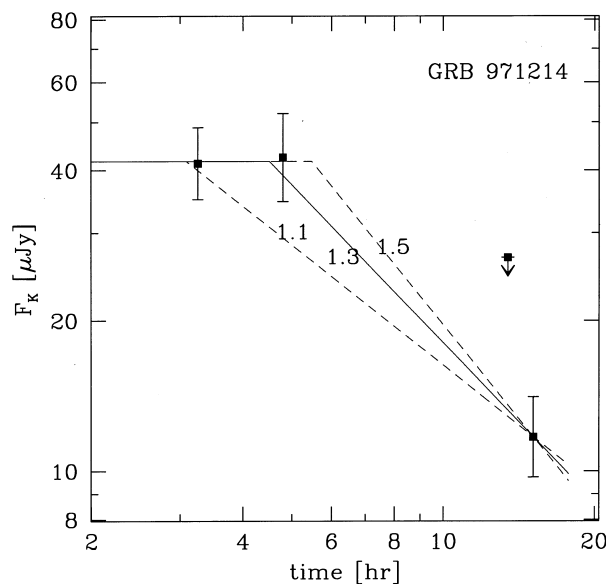


FIG. 3.—*K* flux of GRB 971214 as a function of time. Extrapolations to early times of the Keck measurement after 14 hr (Kulkarni et al. 1998) are shown for the same three values of δ used in Fig. 4. Other data are by Gorosabel et al. (1998) and Garcia et al. (1997; the upper limit). The assumption here is that *K* lies above ν_m and below ν_c (the situation in the right-hand panel of Fig. 4). Therefore, the actual slope of each curve is 0.25 less than the value of δ (by which it is labeled) because *K* lies below the cooling break, and δ is measured in *VRI*, above the cooling break, where the temporal slope is steeper by $1/4$ than below it.

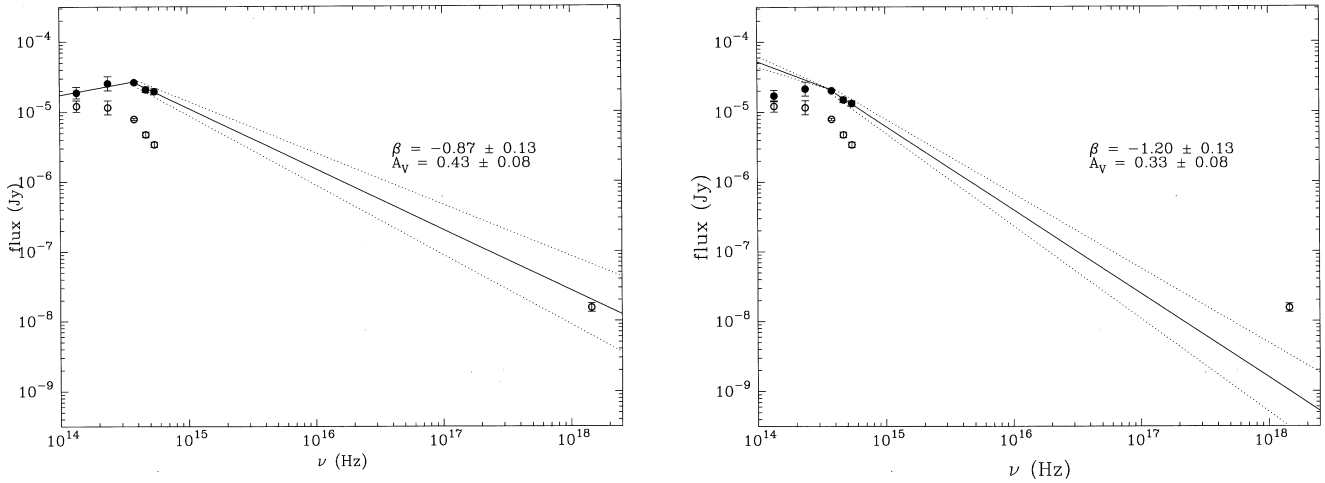


FIG. 4.—Near-infrared/optical-to-X-ray spectral flux distribution of GRB 971214 on December 15.50 UT (the epoch of the I -band measurement). Open symbols indicate the measured values (from Ramaprakash et al. 1998 and Heise et al. 1999) extrapolated to December 15.50 UT. Note that the error on the J -band data is much larger than used by Ramaprakash et al. (1998), in agreement with the original report (Tanvir et al. 1997). Filled symbols indicate the dereddened data. The dotted lines indicate the 1σ errors on the spectral slope as derived from the temporal slope. *Left*: Result of assuming that the break is the synchrotron peak. The spectrum below the peak follows the low-frequency tail of the synchrotron spectrum, where $F_\nu \propto \nu^{1/3}$. *Right*: Result of assuming that the break is the cooling break. The spectral slope changes by 0.5 across the break. The extinction, A_V , derived from the fit, corresponds to the rest-frame V band.

the peak flux of $30\mu\text{Jy}$:

$$\mathcal{E}_{52} = 0.09n^{-1/2} \left(\frac{\epsilon_B}{0.1} \right)^{-1/2}. \quad (34)$$

This value is difficult to reconcile with the energy estimate from ν_m , unless we push the equipartition fractions very close to unity and/or adopt a very low ambient density.

4.2. The Optical Break as ν_c

In order to accommodate the decline in the early K -band flux, we now assume that ν_m was already well below K band at 0.52 days, and therefore the optical break is ν_c . Then the spectral slope in VRI should be related to the temporal decay at those frequencies by $\beta = (2\delta + 1)/3$, which for $\delta = 1.3 \pm 0.2$ implies $\beta = 1.2 \pm 0.13$ and $p = 2.4$. This model is explored in the right-hand panel of Figure 4. While it solves the K decline problem, it is a worse fit to the K flux at this time and does not do very well in predicting the X-ray flux, which is 2.3σ above the extrapolated spectrum. Also, if we then say that the IR break is real, we have a peak flux of $60\mu\text{Jy}$. This value is greater than the 8.46 GHz flux limits obtained 0.8–20 days after the burst (Kulkarni et al. 1998). This would require that the self-absorption frequency in this afterglow exceeds 10 GHz. Alternatively, the peak frequency at 20 days could be at least a factor 200 above 8.46 GHz, so that an extrapolation from the peak flux to the radio using an optically thin synchrotron spectrum ($F_\nu \propto \nu^{1/3}$) falls below $10\mu\text{Jy}$. Since we know in this case that ν_m was 1.4×10^{14} Hz after 0.21 days, we can use $\nu_m \propto t^{-3/2}$ to find that $\nu_m = 150$ GHz at 20 days, too low to be compatible with the radio upper limits; we conclude that we must require $\nu_a \gtrsim 10$ GHz, as in the other interpretation of the break, to suppress the radio flux.

Using ν_m and F_m from the IR peak at $t = 5$ hr = 0.21 days, we can again use equations (23) and (26) to get two expressions for the energy in terms of the other unknowns:

$$\mathcal{E}_{52} = 3.0 \left(\frac{\epsilon_e}{0.12} \right)^{-4} \left(\frac{\epsilon_B}{0.089} \right)^{-1} \quad (35)$$

$$\mathcal{E}_{52} = 1.1 \left(\frac{n}{0.030} \right)^{-1/2} \left(\frac{\epsilon_B}{0.089} \right)^{-1/2}. \quad (36)$$

Here we have scaled the unknowns to the values found for GRB 970508. In this case, the two independent energy estimates are quite compatible.

Now that we identified all but the self-absorption frequency in the afterglow of GRB 971214, we may use equations (27)–(30) to get all the parameters of the burst, leaving their dependence on the unknown ν_a explicit. The cooling frequency is $\nu_c = 4 \times 10^{14}$ Hz at 0.52 days. It follows that

$$\mathcal{E}_{52} = 0.46\nu_{a,\text{GHz}}^{-5/6}, \quad n = 0.60\nu_{a,\text{GHz}}^{25/6}, \quad \epsilon_e = 0.26\nu_{a,\text{GHz}}^{5/6}, \quad \epsilon_B = 0.027\nu_{a,\text{GHz}}^{-5/2}. \quad (37)$$

Since we require $\nu_a > 10$ GHz in order to satisfy the radio limits, we get $\mathcal{E}_{52} < 0.07$, $n > 9 \times 10^4$, $\epsilon_e > 1.8$, and $\epsilon_B < 8 \times 10^{-5}$. These values are rather different from those of GRB 970508, and $\epsilon_e > 1.8$ is implausible (but not impossible). With such a low energy and high density, the GRB would become nonrelativistic (and start a faster decline) within about 4 days.

This means that the late-time radio flux may be suppressed without invoking $\nu_a > 10$ GHz, easing the constraints on the parameters somewhat. But with $\nu_a = 1$ GHz we get values for which the GRB remains relativistic for 400 days; this conflicts with the radio limits. We conclude that ν_a probably has to exceed 5 GHz for a consistent solution, implying a fairly low energy and high ambient density for GRB 971214. With a high emitted gamma-ray energy per unit solid angle, $\mathcal{E}_{52\gamma} = 30$, this means that the ratio of emitted gamma-ray energy to remaining energy in the blast wave is uncomfortably large, probably in excess of 100. Either very efficient radiation in the GRB phase of the burst is needed to achieve this or a strong difference in the amount of beaming between the gamma-ray and afterglow emission. Beaming of GRB 971214 to a degree similar to that observed in GRB 990123 (Fruchter et al. 1999b; Kulkarni et al. 1999) would allow a more standard solution for the parameters: all the trouble arises from the fact that the radio limits force a high ν_a . If the burst was beamed so that it started declining more sharply after a day or so, then the radio flux at later times could be naturally low, and we would be allowed to choose $\nu_a \sim 1$ GHz, which leads to parameter values for GRB 971214 that are similar to those of GRB 970508. It would even open the possibility that the temporal decay is somewhat contaminated by the steeper decay after the beaming break, so we should have used a slightly shallower temporal and spectral slope in fitting the spectrum of GRB 971214 at 0.52 days with a cooling break. Then both the X-ray and K flux would agree much better with the fit. However, this now is a little too much speculation for the amount of data available, and it may well be wrong to try to bring the parameters of GRB 971214 into agreement with those of GRB 970508. We already know that afterglows are diverse. For example, GRB 980703 had a cooling break in X rays after a day rather than in the optical (Vreeswijk et al. 1999; Bloom et al. 1998b). We simply need more well-measured bursts in order to establish the allowed ranges of parameters such as ϵ_e and ϵ_B .

In summary, neither the identification of the optical break as ν_m nor as ν_c is without problems, so we should take any derived parameters for this burst with a grain of salt. But the ν_m interpretation is in our view the least tenable, since it predicts that the flux at K should have risen from the start until about a day after the burst, whereas the data clearly show a declining K flux. The problem of the ν_c interpretation is that the X-ray flux at 0.52 days is about 2.3σ higher than expected, and the K -band flux lower, which is somewhat uncomfortable but perhaps tolerable.

5. CONCLUSION

We have calculated the synchrotron spectra from the blast waves causing GRB afterglows and derive improved expressions for the relations between measured break frequencies and the intrinsic properties of the blast wave. These allow us to relate the blast wave properties to observable quantities more accurately. We correct the expression for the blast wave energy by almost 2 orders of magnitude. Our expressions are exact for an undecelerated, uniform medium. Deceleration and radial structure of the shock are expected to change the expressions for the final parameters by another factor of a few, much less than the corrections found here but still of interest. Combined with the uncertainties in the measured values of the spectral breaks and fluxes, this means that the blast wave parameters derived here are still uncertain by an order of magnitude (see the solution by Granot, Piran, & Sari 1998 as an illustration of the possible differences).

There are enough data on GRB 970508 to compute all intrinsic parameters of the blast wave. The energy in the blast wave is 3×10^{52} ergs/ 4π sr. The ambient density into which the blast wave expands is 0.03 cm^{-3} , on the low side for a disk of a galaxy. The fraction of postshock energy that goes into electrons is 12%, and that into magnetic field, 9%. We also estimate the fraction of energy transferred to electrons during the gamma-ray phase and find this to be 15%. The agreement with the later blast wave value suggests that the fraction of energy given to electrons is constant from 10 s to 10^6 s after the trigger.

For GRB 971214 there is ambiguity in the interpretation of the break seen in the optical a half-day after the burst. We argue that the break is most likely to be the cooling break, but the argument is not watertight. Assuming it is the cooling break, we still lack the self-absorption frequency, but radio limits constrain this to be in excess of about 5 GHz. The limits on parameters that follow from this indicate that the afterglow properties of GRB 971214 are different from those of GRB 970508. GRB 971214 must either have had more narrow beaming in gamma rays than in optical or have radiated its initial energy with more than 99% efficiency in the gamma-ray phase, according to the parameters we derive. Also its magnetic field was far below equipartition, $\epsilon_B \lesssim 10^{-4}$. However, beaming or other additions could ease the constraints and allow parameter values similar to those of GRB 970508, so the physical parameters of GRB 971214 are very poorly constrained.

Our analysis emphasizes the importance of early measurements covering a wide range of wavelengths. The full identification of the cooling frequency ν_c in GRB 970508 hinged on abundant photometry, including colors, being available soon after the burst, since the break passed R after 1.5 days (Galama et al. 1998b). In H and K , the action lasted a week (Galama et al. 1998b), and this is the general trend: there is more time in IR, since all breaks pass later there. However, our revised coefficient for the peak frequency, ν_m , shows that the peak can only be caught in the IR within hours of the trigger (or much later in the radio). A case in point are the very early K' -band measurements of GRB 971214 by Gorosabel et al. (1998), which provide an invaluable constraint on this afterglow as they may have caught the passage of ν_m through K' . Therefore, we encourage first and foremost early long-wavelength coverage, including searches for afterglows in IR, as a method of effectively constraining afterglow parameters. Two of the three crucial break frequencies in an afterglow can pass the optical and IR within hours and days, respectively. There is no time first to search and only then to attempt broad coverage. Instantaneous alerts from HETE2 and SWIFT will therefore greatly advance our understanding of afterglow physics. For HETE2, and to some extent for SWIFT, this will require an enormous amount of work from a network of ground-based observatories with good coverage in longitude and latitude, so that always at least one observatory is well placed for immediate response.

R. A. M. J. Wijers was supported for part of the work by a Royal Society URF grant. T. J. Galama is supported through a grant from NFRA under contract 781.76.011. We thank Jules Halpern for alerting us to the X-ray data on GRB 971214 and pointing out that our original model was inconsistent with the X-ray flux.

REFERENCES

- Blandford, R. D., & McKee, C. F. 1976, *Phys. Fluids*, 19, 1130
 Bloom, J. S., Djorgovski, S. G., Kulkarni, S. R., & Frail, D. A. 1998a, *ApJ*, 507, L25
 Bloom, J. S., et al. 1998b, *ApJ*, 508, L21
 Bond, H. E. 1997, *IAU Circ.* 6654
 Brainerd, J. J. 1998, *ApJ*, 496, L67
 Castro-Tirado, A. J., Gorosabel, J., Galama, T., Groot, P., van Paradijs, J., & Kouveliotou, C. 1998, *IAU Circ.* 6848
 Costa, E., et al. 1997a, *IAU Circ.* 6649
 ———. 1997b, *Nature*, 387, 783
 Frail, D. A., Kulkarni, S. R., Nicastro, L., Feroci, M., & Taylor, G. B. 1997, *Nature*, 389, 261
 Frontera, F., et al. 1991, *Adv. Space Res.*, 11, 281
 ———. 1998, *A&A*, 334, L69
 Fruchter, A., Livio, M., Macchetto, D., Petro, L., Sahu, K., Pian, E., Frontera, F., Thorsett, S., & Tavani, M. 1997, *IAU Circ.* 6747
 Fruchter, A. S., et al. 1999a, *ApJ*, 519, L13
 Fruchter, A. S., et al. 1999b, *ApJ*, submitted (astro-ph/9902236)
 Galama, T. J., et al. 1998a, *ApJ*, 500, L101
 Galama, T. J., Wijers, R. A. M. J., Bremer, M., Groot, P. J., Strom, R. G., Kouveliotou, C., & van Paradijs, J. 1998b, *ApJ*, 500, L97
 Garcia, M. R., Muench, A., Tollestrup, E., Callanan, P. J., & McCarthy, J. 1997, *IAU Circ.* 6792
 Gorosabel, J., et al. 1998, *A&A*, 335, L5
 Granot, J., Piran, T., & Sari, R. 1998, *ApJ*, 513, 679
 Halpern, J. P., Thorstensen, J. R., Helfand, D. J., & Costa, E. 1998, *Nature*, 393, 41
 Heise, J., et al. 1997a, *IAU Circ.* 6654
 ———. 1997b, *IAU Circ.* 6787
 ———. 1999, in preparation
 Jager, R., Heise, J., in 't Zand, J., & Brinkman, A. C. 1995, *Adv. Space Res.*, 13, 315
 Katz, J. I., & Piran, T. 1997, *ApJ*, 490, 772
 Kippen, M. R., Woods, P., Connaughton, V., Smith, D. A., Levine, A. M., & Hurley, K. 1997, *IAU Circ.* 6789
 Kouveliotou, C., Briggs, M. S., Preece, R., Fishman, G. J., Meegan, C. A., & Harmon, B. A. 1997, *IAU Circ.* 6660
 Kulkarni, S. R., et al. 1998, *Nature*, 393, 35
 ———. 1999, *Nature*, in press
 Mészáros, P., & Rees, M. J. 1997, *ApJ*, 476, 232
 Metzger, M. R., Cohen, J. G., Chaffee, F. H., & Blandford, R. D. 1997a, *IAU Circ.* 6676
 Metzger, M. R., Djorgovski, S. G., Kulkarni, S. R., Steidel, C. C., Adelberger, K. L., Frail, D. A., Costa, E., & Frontera, F. 1997b, *Nature*, 387, 879
 Panaitescu, A., & Mészáros, P. 1998, *ApJ*, 493, L31
 Pian, E., et al. 1998, in *AIP Conf. Proc.* 428, Fourth Huntsville Gamma-ray Burst Symposium, ed. C. Meegan, R. Preece, & T. Koshut (New York: AIP), 504
 Piro, L., et al. 1997, *IAU Circ.* 6656
 Piro, L., Scarsi, L., & Butler, R. C. 1995, *Proc. SPIE* 2517, 169
 Ramaprakash, A. N., et al. 1998, *Nature*, 393, 43
 Rees, M. J. 1966, *Nature*, 211, 468
 Rees, M. J., & Mészáros, P. 1992, *MNRAS*, 258, L41
 Reichart, D. E. 1997, *ApJ*, 485, L57
 Rhoads, J. E. 1998, *ApJ*, submitted (astro-ph/9903399)
 Rybicki, G. B., & Lightman, A. P. 1979, *Radiative Processes in Astrophysics* (New York: John Wiley & Sons)
 Sari, R. 1998, *ApJ*, 494, L49
 Sari, R., Piran, T., & Narayan, R. 1998, *ApJ*, 497, L17
 Tanvir, N., Wyse, R., Gilmore, G., & Corson, C. 1997, *IAU Circ.* 6796
 van Paradijs, J., et al. 1997, *Nature*, 386, 686
 Vreeswijk, P. M., et al. 1999, *ApJ*, 523, 171
 Waxman, E. 1997a, *ApJ*, 491, L19
 ———. 1997b, *ApJ*, 485, L5
 Wijers, R. A. M. J., Rees, M. J., & Mészáros, P. 1997, *MNRAS*, 288, L51